Since January 2020 Elsevier has created a COVID-19 resource centre with free information in English and Mandarin on the novel coronavirus COVID-19. The COVID-19 resource centre is hosted on Elsevier Connect, the company's public news and information website.

Article

Cell Host & Microbe

Viral Nucleases Induce an mRNA Degradation-Transcription Feedback Loop in Mammalian Cells

Graphical Abstract

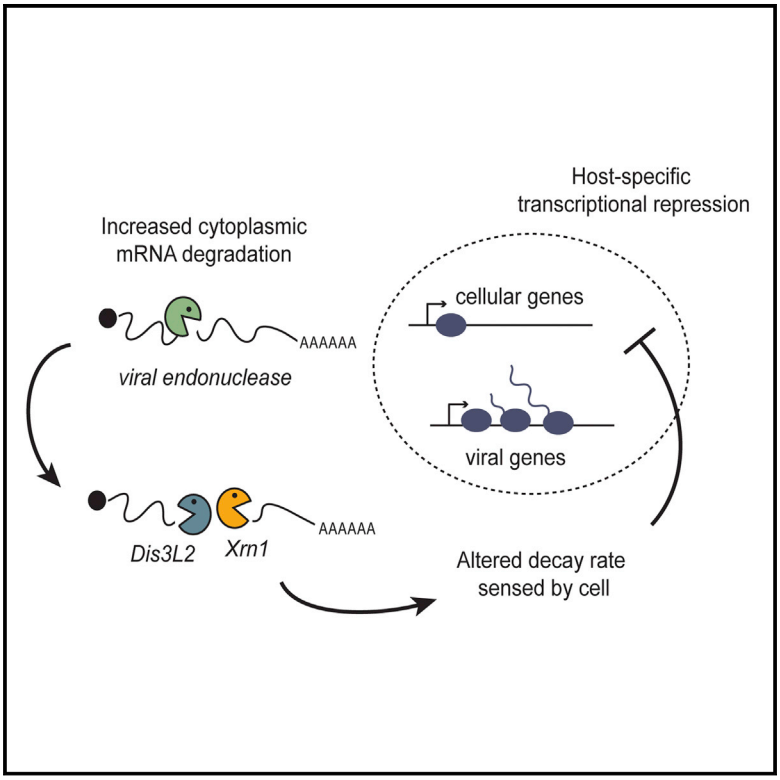

Authors

Emma Abernathy, Sarah Gilbertson, Ravi Alla, Britt Glaunsinger

Correspondence

glaunsinger@berkeley.edu

In Brief

Gamma-herpesviruses encode an endonuclease that induces cellular mRNA degradation. Abernathy et al. show that viral nuclease-triggered mRNA decay leads to repression of cellular transcription and decreased RNA Polymerase II (RNAPII) recruitment. RNAPII-transcribed viral genes escape this transcriptional repression, highlighting how viruses use this mRNA decay-transcription feedback mechanism for their benefit.

Highlights

- Herpesvirus-induced cytoplasmic mRNA decay causes transcriptional alterations
- The mRNA decay-transcription feedback mechanism requires cellular decay factors
- Herpesviral genes escape mRNA degradation-induced transcriptional repression

Accession Numbers

GSE70481
GSM1782681
GSM1782682
GSM1782683
GSM1782684
GSM1782685
GSM1782686

Abernathy et al., 2015, Cell Host & Microbe *18*, 243–253
August 12, 2015
http://dx.doi.org/10.1016/j.chom.2015.06.019

Cell Host & Microbe
Article

Viral Nucleases Induce an mRNA Degradation-Transcription Feedback Loop in Mammalian Cells

Emma Abernathy,[1] Sarah Gilbertson,[2] Ravi Alla,[3] and Britt Glaunsinger[1,2,*]
[1]Department of Plant and Microbial Biology, University of California, Berkeley, CA 94720, USA
[2]Department of Molecular and Cell Biology, University of California, Berkeley, CA 94720, USA
[3]QB3 Computational Genomics Resource Laboratory, University of California, Berkeley, CA 94720, USA
*Correspondence: glaunsinger@berkeley.edu
http://dx.doi.org/10.1016/j.chom.2015.06.019

SUMMARY

Gamma-herpesviruses encode a cytoplasmic mRNA-targeting endonuclease, SOX, that cleaves most cellular mRNAs. Cleaved fragments are subsequently degraded by the cellular 5′-3′ mRNA exonuclease Xrn1, thereby suppressing cellular gene expression and facilitating viral evasion of host defenses. We reveal that mammalian cells respond to this widespread cytoplasmic mRNA decay by altering RNA Polymerase II (RNAPII) transcription in the nucleus. Measuring RNAPII recruitment to promoters and nascent mRNA synthesis revealed that the majority of affected genes are transcriptionally repressed in SOX-expressing cells. The transcriptional feedback does not occur in response to the initial viral endonuclease-induced cleavage, but instead to degradation of the cleaved fragments by cellular exonucleases. In particular, Xrn1 catalytic activity is required for transcriptional repression. Notably, viral mRNA transcription escapes decay-induced repression, and this escape requires Xrn1. Collectively, these results indicate that mRNA decay rates impact transcription and that gamma-herpesviruses use this feedback mechanism to facilitate viral gene expression.

INTRODUCTION

Viruses are extensively integrated into the cellular gene expression network, having evolved strategies to alter or co-opt machinery involved in the stages of transcription and RNA fate through translation and protein turnover. As such, they have served as valuable tools to dissect the pathways that govern cellular gene expression. Though gene expression is often considered in terms of a unidirectional flow of discrete events, there are an increasing number of examples of how these basic stages are interconnected (Braun and Young, 2014; Huch and Nissan, 2014). Such feedback mechanisms may enable cells to maintain homeostasis or mount appropriate responses during periods of perturbation. Viral infections represent a significant stress for the cell and thus are likely to alter or stimulate crosstalk between components of the gene expression cascade.

Recent work has revealed that a feedback loop exists between mRNA synthesis and degradation in *S. cerevisiae* (Haimovich et al., 2013; Sun et al., 2013). One of the key proteins involved in linking mRNA decay to transcription is the 5′-3′ mRNA exonuclease Xrn1, which is the primary exonuclease involved in cytoplasmic mRNA degradation in *Drosophila*, yeast, and mammals (Nagarajan et al., 2013). However, although the data are consistent that Xrn1 deletion impacts mRNA synthesis in yeast, reports differ both as to the specific requirement for Xrn1, as well as whether it serves as a direct or indirect transcriptional regulator (Haimovich et al., 2013; Sun et al., 2013).

Whether similar cytoplasmic mRNA decay-transcription feedback mechanisms are operational in higher eukaryotes such as mammals remains unknown. Furthermore, how enhanced mRNA degradation might signal through such a feedback loop is an open question and one that is difficult to address through mutant studies. In this regard, several mammalian viruses rapidly accelerate cytoplasmic mRNA degradation through the combined activity of virally encoded mRNA-targeting endonucleases and mammalian Xrn1 and thus could provide insight into these questions (Gaglia et al., 2012). Members of the alpha- and gamma-herpesvirus subfamilies, as well as influenza A virus (IAV) and SARS coronavirus (SCoV), all encode viral proteins that target mRNAs for endonucleolytic cleavage (Glaunsinger and Ganem, 2004; Jagger et al., 2012; Kamitani et al., 2009; Kwong and Frenkel, 1987; Rowe et al., 2007). Though the viral proteins are not homologous, in all examined cases they bypass the rate-limiting deadenylation and decapping events by inducing internal cleavages in cytoplasmic mRNA, and then rely on the cellular mRNA decay machinery to degrade the cleaved mRNA fragments. For the alpha- and gamma-herpesviruses and SCoV, clearance of cleaved mRNAs requires Xrn1 (Covarrubias et al., 2011; Gaglia et al., 2012).

Here, by comparing the effects of gamma-herpesviruses that contain wild-type or inactivated mRNA-targeting nucleases, we reveal a direct connection between accelerated cytoplasmic mRNA decay and altered RNA Polymerase II (RNAPII) transcription in mammalian cells. However, contrary to what might be predicted based on observations in *S. cerevisiae*, we find that enhancing mRNA degradation leads predominantly to a decrease in RNAPII activity on cellular genes, although a subset of genes are transcriptionally upregulated. We show a central

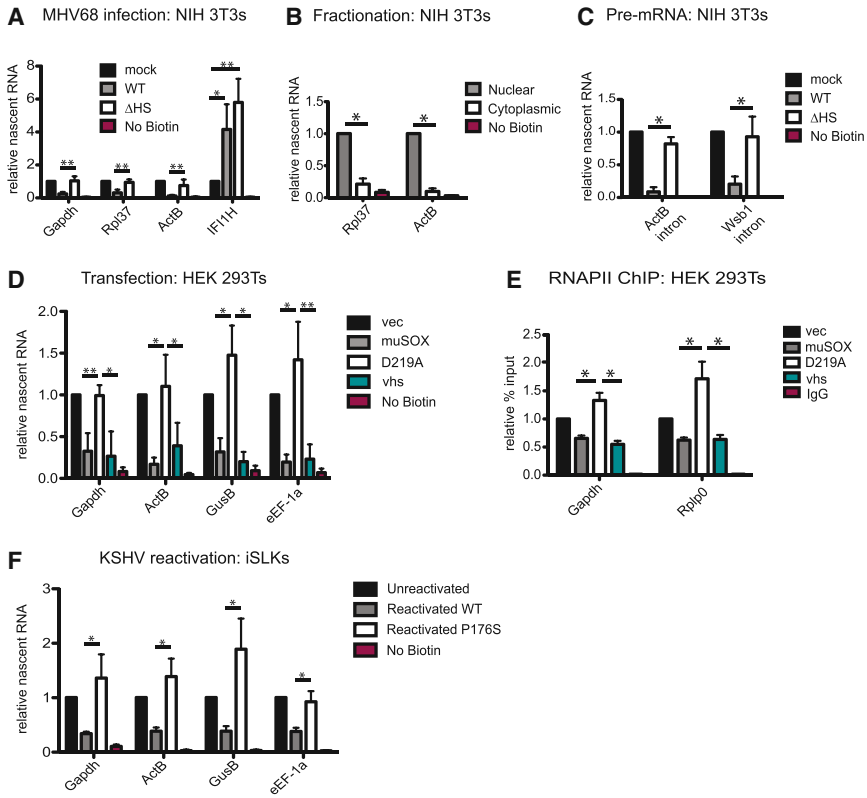

Figure 1. Enhanced mRNA Turnover in the Cytoplasm Suppresses RNAPII Transcription

(A) NIH 3T3 cells were infected with WT or ΔHS MHV68 for 24 hr, whereupon 500 μM of 4sU was added for 30 min and labeled RNA was isolated by biotin-streptavidin pull-down. Levels of newly transcribed RNA were measured by RT-qPCR. All samples were normalized to 18S, and mock-infected levels were set to 1.

(B) 4sU was added to NIH 3T3 cells for 30 min, followed by fractionation into nuclear and cytoplasmic fractions. Purified 4sU-labeled RNA was quantified by RT-qPCR for the indicated genes.

(C) NIH 3T3 cells were infected with MHV68 for 24 hr and 4sU-labeled for 30 min. RNA was quantified as above using intron-specific primers.

(D) HEK293T cells were transfected with the indicated plasmids for 24 hr, then labeled with 4sU for 30 min prior to RNA purification and quantification by RT-qPCR.

(E) HEK293T cells were transfected as above for 24 hr, and cells were crosslinked prior to analysis of RNAPII occupancy at the indicated promoters by ChIP followed by qPCR. No antibody was added to the IgG sample.

(F) iSLK cells latently infected with WT or P176S KSHV were reactivated for 48 hr with dox and sodium butyrate. 4sU was added for 30 min, and labeled RNA was isolated and quantified by RT-qPCR. Error bars represent the mean with SEM of $\geq$ 3 independently performed experiments. Student's t test was used to determine statistical significance. *p $\leq$ 0.05, **p $\leq$ 0.005, ***p $\leq$ 0.0005.

role for cellular exonucleases including Xrn1 in this repression, indicating that Xrn1-linked transcriptional regulation is a feature conserved between *S. cerevisiae* and mammals. Furthermore, our findings support the conclusion that it is the act of mRNA degradation by cellular nucleases that is sensed and triggers transcriptional alterations, rather than secondary effects from stabilization of mRNAs encoding transcriptional regulators. Interestingly, viral transcription, which is also mediated by RNAPII, largely escapes transcriptional repression.

RESULTS

Enhanced mRNA Turnover in the Cytoplasm Suppresses RNAPII Transcription

Infection with murine gamma-herpesvirus 68 (MHV68) leads to widespread acceleration of mRNA decay in the cytoplasm that is initiated by mRNA cleavage by the viral endoribonuclease muSOX and completed by degradation of the cleaved fragments by the cellular 5′-3′ exoribonuclease Xrn1 (Covarrubias et al., 2009; Gaglia et al., 2012). A point mutation in the muSOX gene at position R443 (R443I; ΔHS) renders it defective for cleaving cytoplasmic RNAs, and thus infection with the ΔHS virus does not broadly increase mRNA decay (Richner et al., 2011). We therefore queried how infection of NIH 3T3 cells with WT MHV68 versus the ΔHS mutant impacted rates of cellular mRNA transcription as measured by 4-thiouridine (4sU) pulse labeling. Just prior to harvesting, mock-infected or infected cells were incubated for 30 min with 4sU, which gets incorporated into actively transcribing mRNAs and can be subsequently coupled to HPDP-biotin and purified over magnetic streptavidin beads. Quantification by RT-qPCR of the housekeeping genes Gapdh, Rpl37, and ActB from purified 4sU-labeled RNA showed a significant transcriptional reduction during MHV68 infection compared to mock-infected cells (Figure 1A). No reduction in transcription was detected in cells infected with the ΔHS point mutant virus, suggesting that the transcriptional suppression observed during WT MHV68 infection was specifically linked to enhanced cytoplasmic mRNA decay (Figure 1A). We detected robust transcriptional activation during both MHV68 WT and ΔHS infection of the interferon-stimulated gene IFIH1 (Liu et al., 2012), indicating the 4sU assay accurately portrays transcription changes. We applied several tests to confirm that the abundance of 4sU-containing mRNA reflected nascent transcription rather than decay rates in the cytoplasm. First, we showed that 4sU-labeled mRNA remained largely confined to the nucleus at the time of harvest (Figure 1B). Second, we also quantified the 4sU-labeled RNA using primers within intronic sequences, confirming that the transcriptional repression was observed for pre-mRNA (Figure 1C). Finally, we observed similar transcriptional repression when applying only a 5-min 4sU pulse, and normalizing each sample to the number of cells harvested after 4sU addition confirmed nascent RNA levels are altered only during a WT infection (Figures S1A and S1B).

To test directly whether the transcriptional alterations that occurred during MHV68 infection were due to accelerated mRNA decay, we examined whether this phenotype could be

recapitulated upon expression of the viral endonuclease alone. HEK293T cells were transfected with plasmids expressing WT muSOX, the catalytically dead point mutant muSOX D219A, or the viral endonuclease vhs from herpes simplex virus (HSV-1). Although not homologous to muSOX, HSV-1 vhs is also a broad-acting, cytoplasmic, mRNA-specific endonuclease that engages Xrn1 to degrade the cleaved RNA fragments (Gaglia et al., 2012; Read, 2013). Similar to our results in infected cells, 4sU labeling showed a reduction of transcription of the housekeeping genes Gapdh, ActB, GusB, and eEF-1a in cells expressing muSOX or vhs, but not in cells expressing the muSOX D219A mutant (Figure 1D). We also measured RNAPII occupancy at cellular promoters by chromatin immunoprecipitation (ChIP) assays and, in agreement with our 4sU labeling, observed a reduction in RNAPII occupancy in cells expressing vhs or muSOX but not muSOX D219A (Figure 1E).

Finally, we performed a similar set of experiments with the human gamma-herpesvirus Kaposi's sarcoma-associated herpesvirus (KSHV). KSHV encodes a SOX gene that functions in a manner analogous to MHV68 muSOX (Covarrubias et al., 2009; Glaunsinger and Ganem, 2004). We engineered a P176S point mutation in the KSHV SOX gene, which, similar to the MHV68 ΔHS mutant, confers a specific mRNA degradation defect (Glaunsinger et al., 2005). We monitored mRNA degradation-induced transcriptional changes during the lytic KSHV replication cycle using iSLK renal carcinoma cells, which harbor a doxycycline (dox)-inducible version of the major lytic cycle transactivator RTA and can be stimulated to replicate the virus upon treatment with dox and sodium butyrate (Myoung and Ganem, 2011). Measurement of transcription rates 48 hr post-lytic reactivation by 4sU labeling showed a specific transcriptional repression of the housekeeping genes Gapdh, ActB, GusB, and eEF-1a in cells containing WT KSHV but not the P176S mutant (Figure 1F). Collectively, these data suggest that virus-induced cytoplasmic mRNA degradation induces RNAPII transcriptional repression.

Cellular Exonucleases Are Required for the mRNA Decay-Transcription Feedback Mechanism

We next sought to determine what cellular factor(s) were required to activate the mRNA decay-induced transcriptional feedback mechanism. Given that Xrn1 degrades the mRNA fragments cleaved by the viral endonucleases, we reasoned that Xrn1 activity might be involved in the transcriptional response to mRNA degradation in mammalian cells. We generated HEK293T cells stably expressing dox-inducible Xrn1-targeting shRNAs. After Xrn1 knockdown by dox treatment for 4 days, the cells were transfected with plasmids expressing either WT or D219A muSOX, and RNAPII promoter occupancy was measured by ChIP. In control cells not treated with dox, we observed the expected reduced RNAPII occupancy at the Gapdh promoter in the presence of WT muSOX, but not the D219A catalytic mutant (Figure 2A). However, Xrn1 knockdown restored RNAPII occupancy at the Gapdh promoter in cells expressing muSOX to levels observed in cells expressing D219A. Importantly, in these experiments mRNAs are cleaved by muSOX regardless of Xrn1 levels. Furthermore, knockdown of Xrn1 in control cells lacking viral nuclease did not result in transcriptional changes by RNAPII ChIP at two cellular promoters (Figure 2B). Thus, it can be concluded that differences in transcription result from a mechanism to sense accelerated mRNA degradation, rather than secondary effects stemming from altered stability of mRNAs encoding transcriptional regulators.

To determine if this effect was specific to Xrn1, we also knocked down three other mammalian factors involved in basal mRNA decay, the 3′-5′ exonuclease Dis3L2 and the deadenylases Ccr4 and Pan2 (Figures 2C and 2E). Although Xrn1 is the only mammalian exonuclease characterized as involved in the degradation of muSOX-cleaved mRNAs, it is likely that 3′-5′ exonucleases also help degrade the cleavage fragments. Similar to the results with Xrn1, depletion of Dis3L2 restored RNAPII occupancy in muSOX-expressing cells to those of control cells (Figure 2C). No effect of Dis3L2 knockdown on RNAPII promoter recruitment was observed in the absence of the viral nuclease (Figure 2D). Finally, although knockdown of Ccr4 alone did not impact the reduction of RNAPII promoter occupancy in muSOX-expressing cells, co-depletion of both Ccr4 and Pan2 restored RNAPII occupancy at the Gapdh promoter (Figure 2E). Unlike our results with Xrn1 and Dis3L2, knockdown of the deadenylases led to an increase in RNAPII promoter occupancy even in the absence of muSOX (Figure 2F), suggesting that in uninfected cells, alterations in deadenylase activity are monitored and drive transcriptional feedback. These data indicate that multiple cellular exonucleases contribute to transcriptional feedback in mammalian cells. Furthermore, in the cases of Xrn1 and Dis3L2, it is their enhanced activity in the presence of widespread mRNA cleavage during infection that is sensed, rather than indirect effects stemming from altered basal mRNA decay.

Xrn1 Catalytic Activity Is Required for Reduced RNAPII Transcription

Because the role of Xrn1 in clearing muSOX-cleaved fragments is well established, we focused on this enzyme and applied a complementation assay to determine if Xrn1 catalytic activity was required for repression of cellular transcription. Cells expressing WT or D219A muSOX were knocked down for endogenous Xrn1 and complemented with plasmids expressing either WT Xrn1 or the catalytically dead mutant D208A (Jinek et al., 2011) (Figure 3A). RNAPII ChIP showed that introduction of WT but not D208A Xrn1 restored the degradation-induced transcriptional repression of the Gapdh promoter in WT muSOX-expressing cells (Figure 3B). This suggests that catalytic activity is required to induce repression of RNAPII transcription and is in agreement with findings in *S. cerevisiae* (Haimovich et al., 2013).

We next explored the possibility that Xrn1 might be directly acting to influence transcription, as has been suggested in yeast (Haimovich et al., 2013). To determine whether Xrn1 translocates to the nucleus in cells undergoing accelerated mRNA decay, we monitored Xrn1 localization during MHV68 infection by immunofluorescence assay (IFA). Although transiently expressed Xrn1 appears to be exclusively cytoplasmic (unpublished data), we observed endogenous Xrn1 in both the nucleus and cytoplasm in NIH 3T3 cells (Figure S2A). The IFA signal was specific for Xrn1, as pre-treatment of the cells with Xrn1-targeting siRNAs significantly decreased the staining in both the nucleus and the cytoplasm (Figure S2A). However, the nuclear-cytoplasmic distribution of Xrn1 was not altered during infection with WT

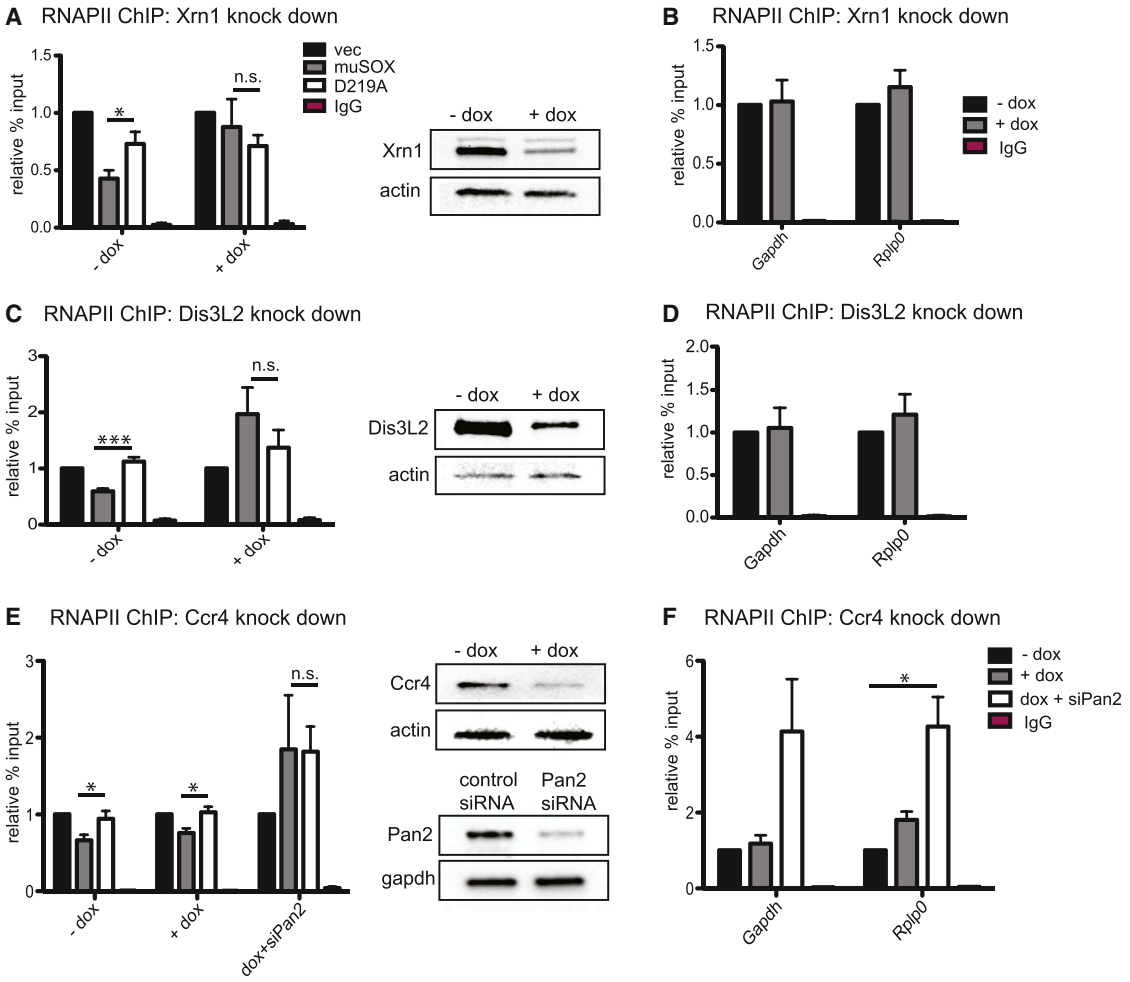

Figure 2. Cellular Exonucleases Are Required for the mRNA Decay-Transcription Feedback Mechanism

(A–E) HEK293T cells with dox-inducible Xrn1, Dis3L2, or Ccr4 shRNAs were mock or dox-treated for 4 days. (A) Xrn1 knockdown cells were transfected with the indicated plasmid for 24 hr. Level of RNAPII at the Gapdh promoter was measured by ChIP followed by qPCR. The level of protein knockdown was assessed by western blot with the indicated antibodies, with actin serving as a loading control. (B) Xrn1 was knocked down in cells lacking the viral nuclease, and RNAPII ChIP was performed at the Gapdh and Rplp0 promoters. (C) RNAPII ChIP at the Gapdh promoter was performed on cells with and without Dis3L2 knockdown. (D) Dis3L2 was knocked down in cells lacking the viral nuclease, and RNAPII ChIP was performed at the Gapdh and Rplp0 promoters. (E) RNAPII ChIP for Gapdh was performed on cells with Ccr4 knockdown, both alone and in combination with siRNA-mediated knockdown of Pan2. (F) Ccr4 was knocked down alone and in combination with Pan2 in cells lacking the viral nuclease, and RNAPII ChIP was performed at the Gapdh and Rplp0 promoters. Error bars represent the mean with SEM of $\geq$ 3 independently performed experiments. *p $\leq$ 0.05, **p $\leq$ 0.005, ***p $\leq$ 0.0005.

MHV68 or the ΔHS mutant (Figures S2B and S2C). We were also unable to detect enrichment of Xrn1 at transcriptionally impacted cellular promoters in ChIP assays (data not shown). These data suggest that it is the sensing of Xrn1 activity in the cytoplasm that leads to transcriptional alterations, rather than a *cis*-acting effect of Xrn1 on cellular promoters.

We next examined whether mRNA decay primarily impacted RNAPII promoter recruitment or elongation. WT MHV68 infection decreased RNAPII promoter occupancy both at the promoter as well as within the gene (Figure 3C), suggesting the transcriptional repression induced by WT MHV68 infection is at least partly due to reduced RNAPII recruitment. Furthermore, the ratio of total to serine-2 (Ser2)-phosphorylated RNAPII (a marker of elongating polymerase; Phatnani and Greenleaf, 2006) was unchanged in response to MHV68 infection of NIH 3T3 cells (Figures 3D and 3E). No alterations in RNAPII occupancy were observed in cells infected with the ΔHS MHV68 (Figure 3D).

We next calculated the transcription elongation rates at three cellular genes using the reversible RNAPII inhibitor 5,6-dichlorobenzimidazole 1-β-d-ribofuranoside (DRB) coupled with 4sU (Fuchs et al., 2014) to measure the speed of polymerase elongation between sites proximal and distal to each promoter (Figure 3E). We observed no significant differences between the elongation rates at the three cellular genes tested in cells infected with WT or ΔHS virus (Figure 3F). Although there was reduced elongation upon infection at the Gapdh gene, this was not linked to mRNA decay, as a similar decrease was observed in the ΔHS-infected cells. Collectively, these data are consistent with RNAPII recruitment being the primary target of mRNA decay-linked transcriptional repression.

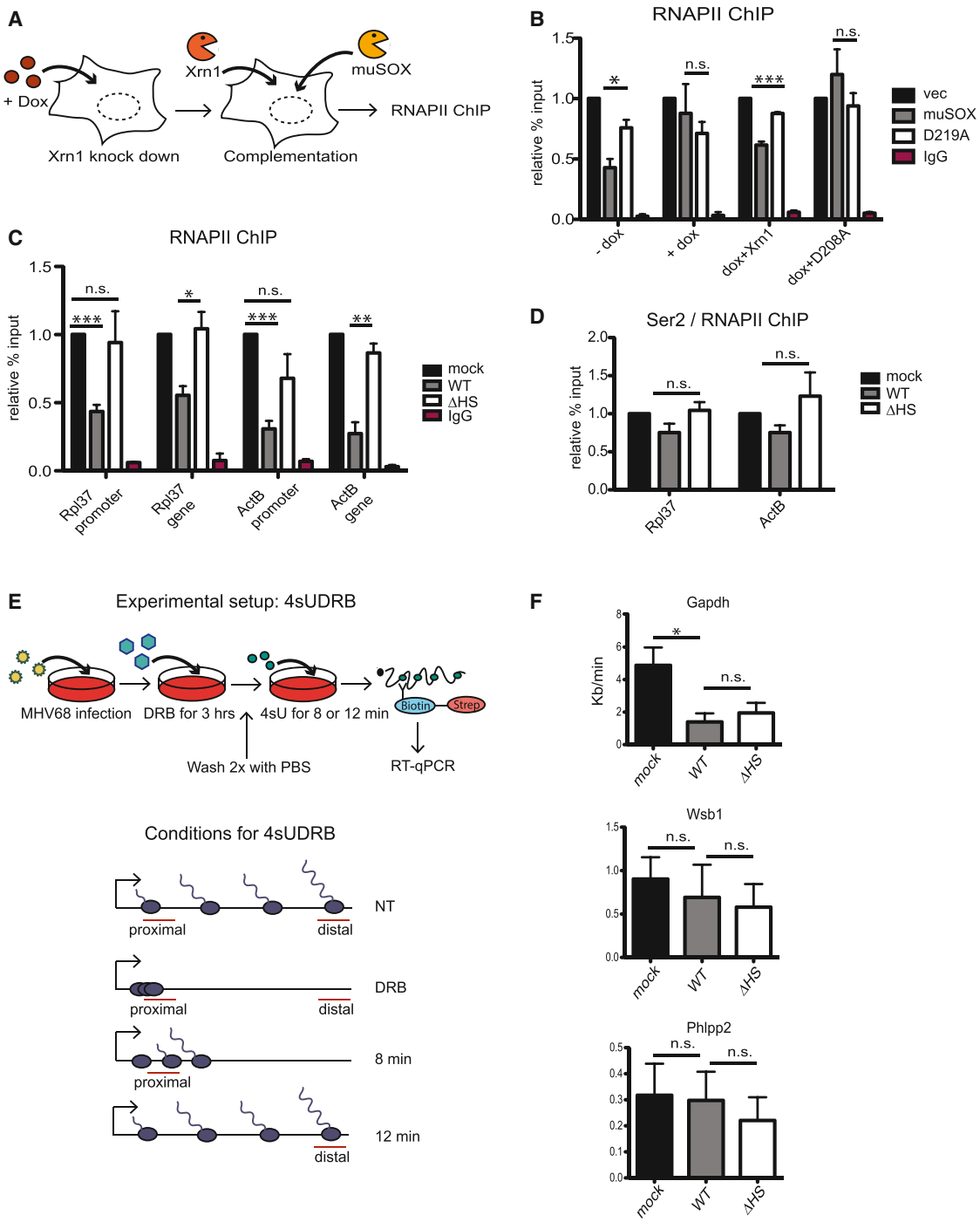

Figure 3. Xrn1 Catalytic Activity Is Required for Reduced RNAPII Transcription

(A) Diagram showing the complementation assay procedure. HEK293T cells with dox-inducible Xrn1 were mock or dox-treated for 4 days, whereupon cells were transfected with plasmids expressing WT or the catalytically dead D208A Xrn1 mutant, as well as with muSOX or muSOX D219A.

(B) Following the above procedure, ChIP and qPCR were performed to measure RNAPII recruitment to the human Gapdh promoter.

(C) NIH 3T3 cells were infected with WT or ΔHS MHV68 for 24 hr. RNAPII recruitment to the Rpl37 and ActB promoters and internal genes was measured by ChIP followed by qPCR.

(D) Ser2 ChIP was performed using the internal Rpl37 and ActB promoters. The level of Ser2-phosphorylated RNAPII was determined by dividing the Ser2 values over the total RNAPII within the same region of the gene.

(E) Diagram showing procedure for calculating transcription elongation rates. DRB was added to infected cells for 3 hr, then removed, and cells were 4sU-labeled. Conditions tested include no DRB treatment (NT), DRB without washout (DRB), 8 min 4sU after DRB washout (8 min), and 12 min 4sU after DRB washout (12 min).

(F) Relative kb/min calculated by normalizing RNA levels to NT and DRB and subtracting the amount of 4sU-labeled RNA at 10 kb (distal) at 12 min from the amount at 1 kb (proximal) at 8 min. Error bars represent the mean with SEM of $\geq$ 3 independently performed experiments. *p $\leq$ 0.05, **p $\leq$ 0.005, ***p $\leq$ 0.0005.

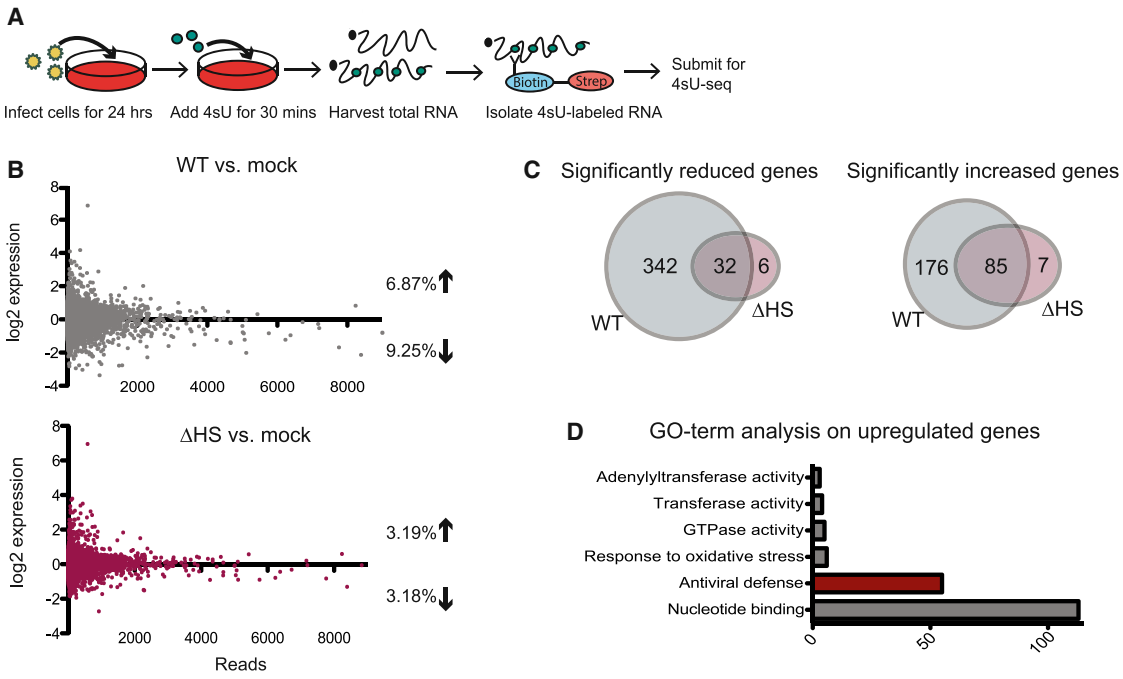

Figure 4. Cellular Transcriptional Changes Occur throughout the mRNA Transcriptome

(A) Libraries were generated from purified 4sU-labled RNA isolated from NIH 3T3 cells infected with WT or ΔHS MHV68 for 24 hr, and sequenced on an Illumina platform.

(B) All genes that aligned to the mouse genome (13,516 genes) were graphed with differential log2 expression values on the y axis and read counts on the x axis. The percentages of genes showing > 1.5-fold increased or decreased expression during infection relative to uninfected cells are indicated.

(C) Venn diagram showing genes that scored as significantly changed during a WT or ΔHS infection, with the overlap region depicting the number of genes significantly reduced or increased in both infections.

(D) Results from a GO-term analysis using DAVID bioinformatics software on the genes found to be increased upon both WT and ΔHS infection.

Cellular Transcriptional Changes Occur throughout the mRNA Transcriptome

To determine the extent of transcriptional alterations that occur in response to accelerated cytoplasmic degradation, we sequenced libraries of 4sU-labeled RNA from mock-, WT-, or ΔHS MHV68-infected NIH 3T3 cells on the Illumina platform (Figure 4A). Relative to uninfected samples, WT MHV68 infection resulted in a ≥ 1.5-fold transcriptional decrease of 9.25% of genes based on log2 fold change (Figure 4B, full list of genes in Table S1). Independent validations of 4sU-labeled mRNA levels by RT-qPCR confirmed the sequencing results for 12 out of 19 genes tested (Figures S3A and S3B). The seven genes in which the two assays were not in agreement showed transcriptional repression by RT-qPCR but not by 4sU-seq, perhaps suggesting that the 4sU-seq represents a conservative estimation of the breadth of degradation-induced transcriptional alterations. Significantly fewer genes (3.18%) were decreased during ΔHS MHV68 infection, indicating that the majority of changes in the WT-infected cells were linked to mRNA degradation. Among the set of transcriptionally repressed genes during WT infection, 374 were categorized as statistically significant based on read counts and fold change. In contrast, only 38 genes were significantly reduced during a ΔHS infection, and among these, 32 overlapped with those in the WT infection samples. Thus, these overlapping genes are likely downregulated as a result of viral infection and are not specific to mRNA degradation (Figure 4C). Gene ontology (GO) term-based analysis of the set of 342 genes that were transcriptionally repressed only during WT MHV68 infection yielded no clear links to specific biological processes (Table S2), suggesting that mRNA degradation-induced transcriptional repression is not restricted to specific functional classes of genes.

Unlike during WT infection, where transcriptional changes were more frequently repressive, the transcriptional changes that occurred during ΔHS infection were equally split between induced and repressed categories (3.19% versus 3.18%, respectively). In addition to the set of transcriptionally repressed genes, we also observed a subset of genes (6.87%) that showed a ≥ 1.5-fold increase upon WT MHV68 infection (Figure 4B). Furthermore, a larger fraction of the significantly transcriptionally induced genes during a WT infection overlapped with those induced during ΔHS infection (32.6% of induced genes compared to 8.6% of reduced genes), suggesting that upregulation is less likely to be linked to mRNA degradation and more likely to be linked to viral infection (Figure 4C). Notably, among the set of 85 genes whose transcriptional induction was common to both WT and ΔHS infection, GO-term analyses returned a clear enrichment for genes involved in antiviral defense mechanisms and in nucleotide binding (Figure 4D). Although the significance of the latter remains to be determined, the induction of antiviral response factors would be a predicted transcriptional response to infection, independent of mRNA degradation.

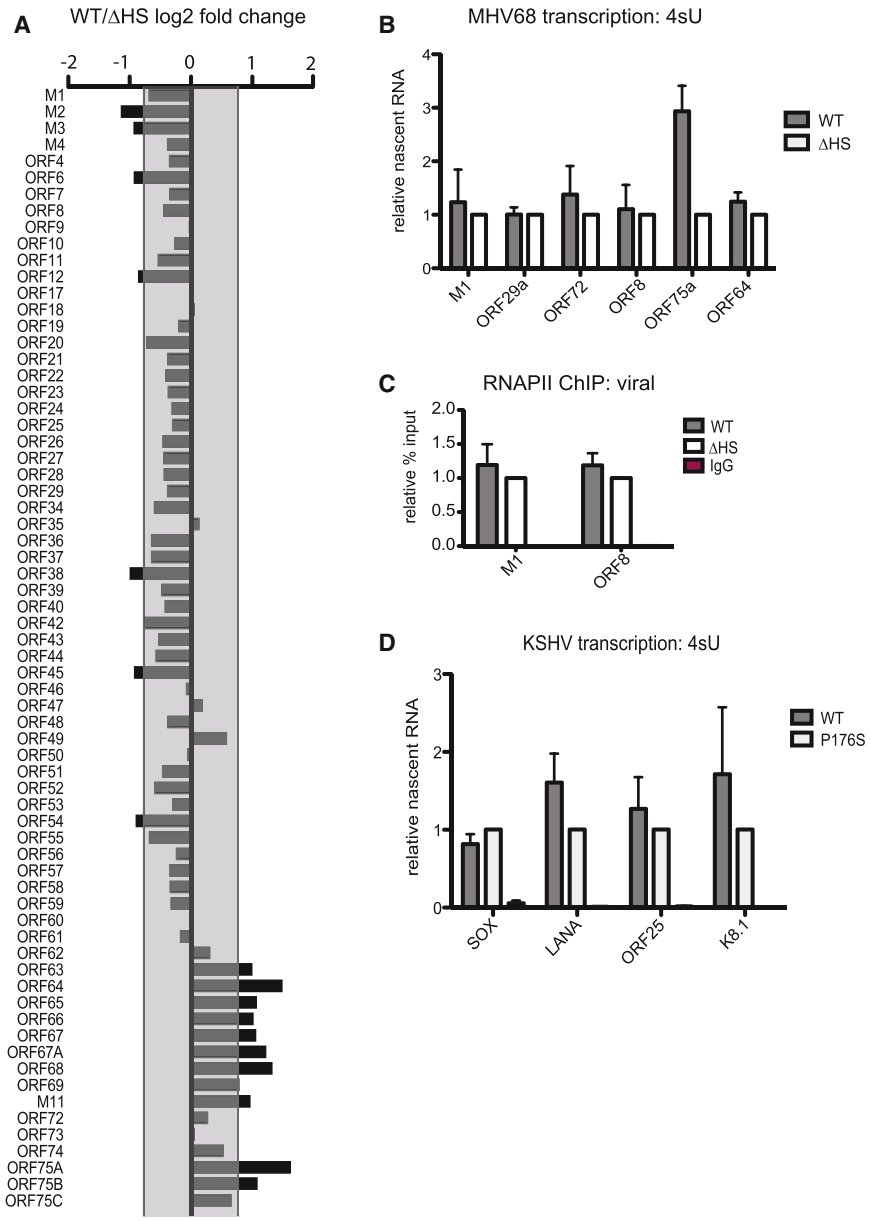

Figure 5. Viral mRNAs Escape Degradation-Induced Transcriptional Repression

(A) 4sU-seq data were used to determine the differential expression of all viral genes between WT and ΔHS infection. Log2 expression changes of WT/ΔHS are shown on the x axis and ORFs are listed in genome order on the y axis. Values outside the shaded box indicate a significant fold change.

(B) Validations of 4sU-seq data by RT-qPCR of purified 4sU-labeled RNA isolated from cells infected with the WT or ΔHS MHV68. Results are normalized to 18S and ΔHS values are set to 1.

(C) ChIP for total RNAPII was performed on NIH 3T3 cells infected with WT or ΔHS MHV68, and the % input values of the viral M1 and ORF8 promoters were compared.

(D) iSLK cells latently infected with WT or P176S KSHV were reactivated for 48 hr with dox and sodium butyrate, then labeled with 4sU for 30 min prior to RNA isolation. RNA levels were compared by RT-qPCR for the indicated viral genes. Error bars represent the mean with SEM of ≥ 3 independently performed experiments.

Viral mRNAs Escape Degradation-Induced Transcriptional Repression

Herpesviral mRNAs are transcribed in the nucleus using the host machinery. We therefore analyzed the transcriptional changes that occurred at each of the viral genes in response to mRNA degradation during WT MHV68 infection relative to ΔHS infection using the 4sU-seq dataset. Interestingly, viral genes largely escaped the transcriptional repression (Figure 5A). Independent validation experiments confirmed that even genes that appeared to undergo modest transcriptional repression during WT infection by 4sU-seq were unchanged or even slightly upregulated as measured by RT-qPCR of 4sU-labeled mRNA (Figure 5B).

In agreement with the 4sU-based transcriptional measurements, we observed no differences in RNAPII occupancy at the M1 and ORF8 viral genes (Figure 5C). Finally, we extended these results to KSHV by comparing viral transcription at 48 hr post-reactivation of WT or P176S KSHV-containing iSLK cells. Similar to the data for MHV68, each of the KSHV genes examined by RT-qPCR following 4sU labeling either exhibited no transcriptional changes or were modestly transcriptionally induced during WT relative to P176S KSHV lytic infection (Figure 5D). We conclude that viral transcription is not negatively impacted (and in some cases is enhanced) by accelerated cytoplasmic mRNA degradation, and thus the transcriptional impact of mRNA decay may be distinct for the virus versus the host.

Xrn1 Positively Influences Viral Transcription during Widespread mRNA Decay

Although the majority of MHV68 genes are susceptible to muSOX cleavage during infection, several viral transcripts appear to escape muSOX-mediated degradation (Abernathy et al., 2014). Two of these putative "escapees," the viral ORF M1 (an RNAPII transcript) and the viral tRNA-like gene vtRNA1 (an RNAPIII transcript), exhibit enhanced steady-state expression during WT relative to ΔHS infection, perhaps due to increased transcription (Abernathy et al., 2014). To test whether muSOX-induced transcriptional feedback was responsible for their increased abundance during WT infection, we first confirmed that the M1 and vtRNA1 half-lives were not altered during a WT versus ΔHS infection (Figure 6A). We then evaluated whether the transcriptional enhancement of these viral genes during WT MHV68 infection was linked to Xrn1 activity using the HEK293T cells expressing dox-inducible Xrn1-targeting shRNAs. Upon Xrn1 knockdown, M1 expression was significantly reduced during WT but not ΔHS MHV68 infection, and its expression was

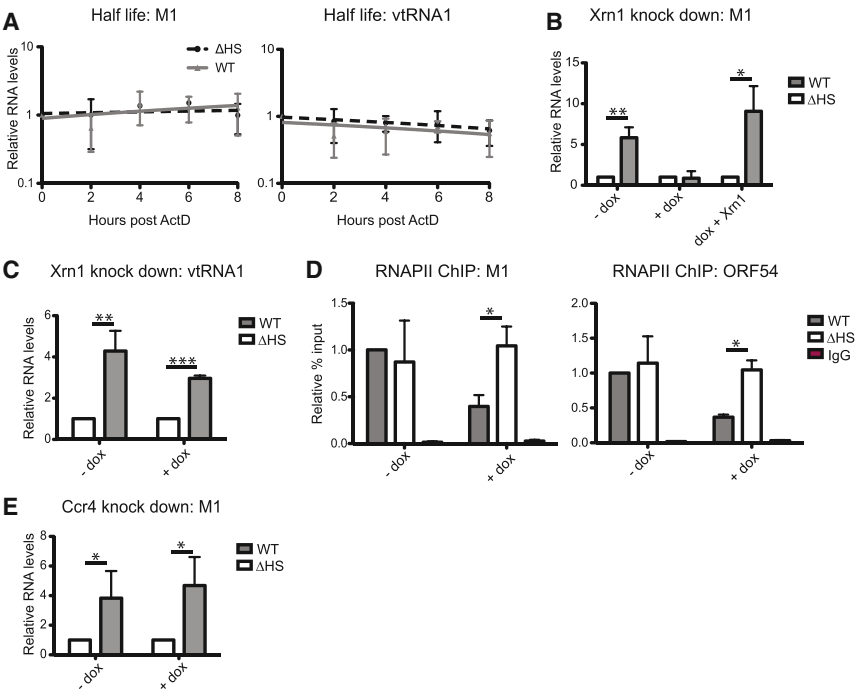

Figure 6. Xrn1 Positively Influences Viral Transcription during Widespread mRNA Decay

(A) NIH 3T3 cells were infected with WT or ΔHS MHV68 for 25 hr, whereupon actinomycin D (ActD) was added to halt transcription, and RNA was harvested at 0, 2, 4, 6, and 8 hr post-addition. RT-qPCR was used to measure the abundance of the viral M1 and vtRNA1 transcripts, and values were normalized to 18S.

(B and C) Complementation assays were performed as described in Figure 3A, except that following 4 days of dox treatment, cells were infected with WT or ΔHS MHV68 for 24 hr. For complementation, exogenous Xrn1 was transfected into the cells prior to MHV68 infection. RT-qPCR was performed for M1 or vtRNA1 on steady-state levels, all samples were normalized to 18S, and ΔHS levels were set to 1 for each condition.

(D) RNAPII ChIP was performed on infected HEK293T cells with or without Xrn1 knockdown. Viral genes M1 and ORF54 were analyzed.

(E) 293T cells containing dox-inducible shRNAs against Ccr4 were mock or dox treated for 4 days, whereupon levels of the viral M1 mRNA were measured by RT-qPCR. Error bars represent the mean with SEM of $\geq$ 3 independently performed experiments. *p $\leq$ 0.05, **p $\leq$ 0.005, ***p $\leq$ 0.0005.

restored upon introduction of exogenous WT Xrn1 (Figure 6B). The requirement for Xrn1 appeared specific for RNAPII-driven transcription, as its depletion had no significant impact on expression of the RNAPIII-transcribed vtRNA1 (Figure 6C). RNAPII ChIP experiments confirmed that the reduction in M1 mRNA in the absence of Xrn1 was due to transcriptional repression (Figure 6D). We also observed reduced RNAPII occupancy upon Xrn1 depletion at ORF54, an MHV68 gene that is susceptible to cleavage by muSOX (Abernathy et al., 2014), indicating that the role of Xrn1 in promoting viral transcription is not limited to transcripts that escape degradation (Figure 6D). In each of these experiments, the requirement for Xrn1 was only observed during WT infection and not during infection with the ΔHS virus. We did not detect any binding of Xrn1 to viral promoters by ChIP (data not shown), suggesting that it likely indirectly impacts viral transcription in cells undergoing enhanced mRNA decay. Finally, depletion of the Ccr4 deadenylase did not alter M1 transcription during a WT or ΔHS infection, in agreement with its dispensability for the repression of cellular transcription when depleted in isolation (Figure 6E). Collectively, these data demonstrate that in contrast to its role in transcriptional repression of many cellular genes, Xrn1 activity during muSOX-induced cytoplasmic mRNA decay is required for robust transcription of viral genes.

DISCUSSION

Here we used virally encoded mRNA-targeting endonucleases to show that cytoplasmic mRNA degradation and nuclear RNAPII transcription are linked in mammalian cells. Accelerated mRNA degradation generally results in transcriptional repression of cellular genes, although there is a subset of genes that are induced. Our findings therefore suggest that mammalian cells have a mechanism to sense broad alterations in RNA degradation. It is not the initial cleavages by viral endonucleases that are detected, but rather the increased activity of cellular exonucleases involved in degrading the cleaved mRNA fragments that generates a transcriptional response. Several cellular exonucleases involved in basal mRNA decay appear central to the transcriptional feedback activated by enhanced mRNA degradation. Notably, enhanced Xrn1 activity appears to have opposing consequences for host and viral transcription, suggesting that herpesviruses have evolved to benefit from this intrinsic feedback mechanism.

Our findings have some clear parallels to gene expression feedback pathways recently described in yeast, although the mammalian response to accelerated mRNA decay does not result in the transcriptional "buffering" phenotype observed in *S. cerevisiae.* In yeast, reducing cytoplasmic mRNA decay through the deletion of components of the mRNA degradation machinery results in a compensatory decrease in RNAPII transcription rates (Haimovich et al., 2013; Sun et al., 2013). Conversely, an RNAPII mutant that exhibits ~3-fold-reduced mRNA synthesis rates displays decreased rates of mRNA turnover in the cytoplasm (Sun et al., 2012). Our data indicate that mammalian cells also possess a mechanism to sense overall mRNA abundance. However, accelerated cytoplasmic mRNA degradation in mammalian cells induces transcriptional alterations that are distinct from this buffering phenotype, in that the majority of mRNA degradation-induced changes involved transcriptional repression. Conversely, our observation that knockdown of the Ccr4 and Pan2 deadenylases increased RNAPII promoter occupancy in uninfected cells suggests that decreased cytoplasmic decay stimulates transcription in mammalian cells. Thus, the transcriptional feedback pathway in mammalian cells appears to operate in a different direction than in yeast. It is notable that in uninfected cells we did not

observe changes in RNAPII occupancy upon depletion of Xrn1 or Dis3L2, perhaps reflecting the ability of alternative exonucleases to compensate for their decreased activity. However, presumably because deadenylation is generally the first and rate-limiting step of basal mRNA decay, stalling that arm of the pathway is sufficient to activate the transcriptional response. Transcriptional repression could represent a way for the cell to conserve energy during stress, or may have evolved as a countermeasure to viral infection, as widespread mRNA decay is more likely to be linked to pathogenesis. If so, gamma-herpesviruses have developed a means to avoid this restriction.

While the subset of transcriptionally repressed genes identified by the 4sU-seq dataset appears smaller than anticipated if this response is global, these results likely represent a conservative estimation of the scope of affected genes. Several genes for which we detected robust decay-induced transcriptional repression by 4sU-RT-qPCR showed more modest effects (or appeared unchanged) in the 4sU-seq data. Possible explanations for this underrepresentation by the 4sU-seq pipeline include the high rates of duplication common to nascent RNA-seq, as well as possible overall lower RNA abundance in cells undergoing widespread mRNA degradation, both of which might mask differential expression. Indeed, when we normalized our 4sU-RT-qPCR data to cell number rather than RNA abundance, we observed an even more dramatic reduction in nascent RNA levels between mock and WT infection.

Our observations linking Xrn1 activity in the cytoplasm to transcriptional alterations complements recent reports in yeast that document a role for Xrn1 in the degradation-transcription feedback loop. Although there is a consensus that Xrn1 is involved in transcription, whether it or the other cellular nucleases operate directly via promoter binding or indirectly by impacting the abundance of mRNAs encoding transcriptional regulators (or by another mechanism) remains to be resolved. Two studies demonstrate that yeast Xrn1 can shuttle into the nucleus and bind cellular promoters to enhance transcription initiation and elongation (Haimovich et al., 2013; Medina et al., 2014). These same studies show that several other cellular decay factors also shuttle into the nucleus and rely on Xrn1 catalytic activity for nuclear import (Haimovich et al., 2013). Another report instead suggests that Xrn1 impacts transcription indirectly in yeast through degradation of mRNAs encoding transcriptional regulators (Sun et al., 2013), although how protein levels would increase upon Xrn1 depletion given that Xrn1 targets deadenylated and decapped messages is unclear. We did not observe a significant increase in the nuclear population of Xrn1 in cells expressing muSOX, nor were we able to detect Xrn1 associated with cellular or viral promoters via ChIP. However, a significant proportion of endogenous Xrn1 resides in the nucleus regardless of viral nuclease expression, hinting that Xrn1 may have nuclear functions in mammalian cells in addition to its well-characterized role in cytoplasmic mRNA decay.

The seemingly opposing roles for Xrn1 in the host and viral transcriptional response may indicate that gamma-herpesviruses benefit from reduced levels of RNAPII occupancy at cellular promoters. One possibility is that degradation-induced cellular transcriptional repression enables the virus to more efficiently recruit polymerases to viral promoters. Indeed, RNAPII is concentrated in herpesviral replication factories in the nucleus (Rice et al., 1994; Sugimoto et al., 2013). However, we did not observe a reduction in virally sequestered RNAPII in cells infected with ΔHS relative to WT MHV68 (unpublished observations), suggesting this cannot fully explain cellular transcriptional repression or viral escape. Alternatively, Xrn1 may more directly impact the transcription of viral promoters in an mRNA decay-dependent manner.

The fact that multiple exonucleases are linked to transcriptional repression is consistent with the idea that the act of mRNA degradation is sensed. Depletion of host exonucleases in cells expressing the viral endonucleases should not impact the overall pool of translationally competent mRNAs, as the mRNAs will still be translationally inactivated by viral endonucleolytic cleavage. However, the cleaved fragments will not be efficiently degraded. Thus, transcriptional changes we observed in mammalian cells should not be due to altered levels of transcriptional regulators, in agreement with the fact that we did not detect alterations in transcription in response to cellular exonuclease depletion in the absence of viral nuclease expression. Instead, we hypothesize that feedback between RNA decay and synthesis may instead be regulated by altered nuclear-cytoplasmic distribution of nucleic acid binding proteins in response to mRNA degradation. For example, yeast polymerase subunits Rpb4/7 shuttle between the nucleus, where they function in transcription, and the cytoplasm, where they are involved in mRNA decay and translation initiation (Harel-Sharvit et al., 2010; Lotan et al., 2007). It may be that factors classically linked to transcription, mRNA decay, and translation function to coordinate and integrate several cellular processes in response to pathogenic or environmental cues (Harel-Sharvit et al., 2010). We propose that this systemic interconnectedness is present in mammalian cells and that viral infections introduce perturbations to mRNA stability whose downstream consequences impact multiple cellular processes.

EXPERIMENTAL PROCEDURES

Cells, Transfections, and Transductions

NIH 3T3 and HEK293T cells were maintained in DMEM (Invitrogen) supplemented with 10% fetal bovine serum (Invitrogen). Cells were transfected at 75%–90% confluence with polyethylenimine for 24 hr. Plasmids pCDNA3-muSOX, pCDNA3-muSOX.D219A, and pCDNA3-vhs have been described previously (Covarrubias et al., 2009; Glaunsinger and Ganem, 2004). Plasmid pFN21-Halo-Xrn1 was kindly provided by Carol Wilusz and subcloned into the pFN21 vector with a FLAG tag. The Xrn1 D208A mutation was introduced by site-directed mutagenesis to generate FLAG-Xrn1.D208A.

HEK293T cells were transduced with TRIPZ inducible lentiviral shRNA constructs (Thermo Scientific) against Xrn1 (clone ID: V2THS_89028), Dis3L2 (clone ID: V3THS_391760), or CNOT6 (clone ID: V2THS_262587). Cells were transfected with shRNA, psPAX2 (lentiviral packaging), and pMD2.G (lentiviral envelope) (Addgene) for 48 hr, whereupon the supernatant was passed through 0.45-μm filters, mixed with 8 μg/ml of polybrene, and spun onto a monolayer of HEK293T cells at 1,500 rpm for 1.5 hr. Fresh media was then added and the cells were incubated for 5–7 days in selection media containing 1 μg/ml puromycin. Cell lines were induced with 1 μg/ml doxycycline for 4–5 days, and knockdown efficiency was determined by western blot and RT-qPCR. Pan2 siRNA (CGGAAUCUCAAUUCCAGAUtt; Life Technologies, ID 113470) was transfected into cells using INTERFERin (PolyPlus) for 48 hr.

Viruses and Infections

The MHV68 bacterial artificial chromosome (BAC) has been described elsewhere (Adler et al., 2000), and the construction of the R443I muSOX mutant

(ΔHS) was previously described (Richner et al., 2011). MHV68 was produced by transfecting NIH 3T3 cells with BAC DNA using SuperFect (QIAGEN). Virus was amplified in NIH 3T12 cells and titered by plaque assay. Cells were infected with MHV68 at an MOI of 5 for 24 hr unless otherwise noted.

KSHV BAC mutagenesis has been described elsewhere (Brulois et al., 2012). The mutant BAC clone was sequenced to confirm the P176S mutation, once after cell line construction, and once after 2 weeks of cell maintenance. KSHV was reactivated by adding 1 μg/ml doxycycline and 1 μg/ml sodium butyrate for 48 hr. Reactivation efficiency was determined by qPCR on isolated DNA and found to be equivalent between WT and P176S.

4sU Labeling

Cells were labeled with DMEM containing 500 μM 4sU (Sigma) for indicated times prior to isolating RNA with TRIzol, followed by isopropanol precipitation. Total RNA (100 μg) was incubated in biotinylation buffer (10 mM Tris [pH 7.4], 1 mM EDTA) and 200 μg HPDP-biotin (EZ-link HPDP-biotin; Thermo Scientific) with constant rotation at room temperature for 1.5 hr. RNA was then phenol-chloroform extracted and precipitated with isopropanol. The pellet was resuspended in DEPC-treated water and mixed with 50 μl Dynabeads MyOne streptavidin C1 (Invitrogen) that had been pre-washed twice with 1X wash buffer (100 mM Tris [pH 7.5], 10 mM EDTA, 1 M NaCl, 0.1% Tween 20). Samples were rotated for 15 min at RT, then washed 3× with 65°C wash buffer and 3× with RT wash buffer. Samples were eluted with 100 μM DTT, and the RNA was precipitated with ethanol prior to RT-qPCR. All qPCR results were normalized to 18S levels and WT or vector control set to 1.

For fractionated 4sU assays, cells were labeled with 4sU as above. Cells were scraped and spun for 10 s at 4°C at max speed. Supernatant was removed and pellet was resuspended in 380 μl ice-cold hypotonic lysis buffer (HLB; 10 mM Tris [pH 7.5], 10 mM NaCl, 3 mM $MgCl_2$, 0.3% NP-40, 10% glycerol). Cells were incubated on ice for 10 min, then vortexed and spun again. The supernatant was collected as the cytoplasmic fraction and the pellet was resuspended in HLB. The cells were washed with HLB 3× and the pellet (nuclear fraction) was resuspended in 1 ml TRIzol and phenol-chloroform extracted. The cytoplasmic fraction was phenol-chloroform extracted and the 4sU protocol continued as described above.

4sU-DRB was performed by adding 100 μM DRB (Sigma) in DMSO for 3 hr, washing 2× with PBS, and adding 4sU for 8 or 12 min. Relative kb/min were calculated by normalizing each time point to the NT sample for mock, WT, and ΔHS infection, followed by a normalization to the DRB sample for mock, WT, and ΔHS to account for background. The number of kb between the 10 kb intronic and 1 kb intronic primer sets was divided by the relative normalized RNA and divided by 4 min for time of elongation.

ChIP

ChIP has been described previously (Listerman et al., 2006), with the following modifications: chromatin was sheared using a Covaris sonicator for 30 rounds of 30 s pulses with 210 V. Chromatin (100 μl) was diluted in 400 μl ChIP dilution buffer containing 10 μg RNAPII antibody (N20-X, Santa Cruz) or Xrn1 (Sigma) and rotated overnight at 4°C. DNA was isolated after reversing the crosslinks using QIAGEN PCR clean up kit prior to qPCR. Each sample was normalized to input.

RT-qPCR

RNA was treated with Turbo DNase (Ambion) and reverse transcribed using AMV RT (Promega) with random 9-mer primers. cDNA was quantified using iTaq Universal SYBR Master Mix (Bio-Rad) and transcript-specific primers. For RNA half-life analyses, 5 μg/μl actinomycin D (Sigma) was added to infected NIH 3T3 cells, and RNA was isolated at the indicated time points and quantified by RT-qPCR. All qPCR results were normalized to 18S levels. All primers used in this study are in Table S3.

4sU RNA-Sequencing

4sU labeled RNA, in duplicate for each sample, was enriched, precipitated, and ribosome depleted (Ribo-Zero). A whole RNA Illumina TruSeq library was then constructed, and 100-bp paired-end sequencing was performed on Illumina HiSeq 2500. Raw reads from the instrument were subjected to adaptor and read quality trimming (Trim Galore, Babraham Institute). Reads were then aligned to the mouse genome (mm10) or to the murine viral genome using TopHat (Trapnell et al., 2009). Gene count tables for known mouse and viral genes were constructed from TopHat2 alignments using htseq-count (Anders et al., 2015). DESeq2 (Love et al., 2014) was then used to estimate pairwise differentially expressed genes. False discovery rate of 10% and log2 ratio of ± 1 were used to filter differentially expressed genes.

GO-term analysis was performed using DAVID bioinformatics resources (v. 6.7) for the induced and reduced gene sets found in both WT- and ΔHS-infected cells (85 and 32 genes, respectively), as well as the genes reduced only during a WT infection (342 genes), and genes only induced during a WT infection (176 genes). A functional annotation chart was generated and sorted by Benjamini false discovery rate of ≤ 0.05.

Western Blots

Dox-inducible cell lines were treated with 1 μg/ml of dox for 5 days, and cell lysates were prepared with lysis buffer (50 mM Tris [pH 7.6], 150 mM NaCl, 3 mM MgCl, 10% glycerol, 0.5% NP-40) and quantified by Bradford assay. Equivalent amounts of each sample were resolved by SDS-PAGE and western blotted with antibodies against Xrn1 (Bethyl; diluted 1:200), Dis3L2 (kindly provided by Torben Jensen; diluted 1:500), Ccr4 (diluted 1:1,000), Pan2 (diluted 1:1,000), and actin (diluted 1:200). Primary antibodies were followed by HRP-conjugated secondary antibodies (Southern Biotechnology, 1:5,000).

ACCESSION NUMBERS

Raw data are available at the NCBI GEO database (GEO: GSE70481). The individual sample accession numbers are GEO: GSM1782681 (mock 1), GEO: GSM1782682 (mock 2), GEO: GSM1782683 (WT MHV68 1), GEO: GSM1782684 (WT MHV68 2), GEO: GSM1782685 (ΔHS MHV68 1), and GEO: GSM1782686 (ΔHS MHV68 2).

SUPPLEMENTAL INFORMATION

Supplemental Information includes Supplemental Experimental Procedures, three figures, and three tables and can be found with this article online at http://dx.doi.org/10.1016/j.chom.2015.06.019.

AUTHOR CONTRIBUTIONS

E.A. and B.G. conceived and designed the experiments. E.A. performed the experiments related to Figures 1, 2, 3, 4, 5, 6, S1, and S3. S.G. performed experiments related to Figures 2 and S2. E.A., S.G., and B.G. analyzed the data. R.A. performed bioinformatics analysis. E.A. and B.G. wrote the paper.

ACKNOWLEDGMENTS

We thank all members of the Glaunsinger lab and Laurent Coscoy for helpful discussions, Ella Hartenien for help with the 4sU DRB experiments, and Carol Wilusz for providing the Xrn1 expression vector. This research was supported by the UC Berkeley Miller Institute, NIH grants R01CA136367 and R01CA160556, a Burroughs Wellcome Fund Investigator in the Pathogenesis of Infectious Disease Award, and a W.M. Keck Foundation Distinguished Young Scientist Award to B.G. The IFA work was performed at the CRL Molecular Imaging Center, supported by Gordon and Betty Moore Foundation.

Received: March 30, 2015
Revised: June 17, 2015
Accepted: June 30, 2015
Published: July 23, 2015

REFERENCES

Abernathy, E., Clyde, K., Yeasmin, R., Krug, L.T., Burlingame, A., Coscoy, L., and Glaunsinger, B. (2014). Gammaherpesviral gene expression and virion composition are broadly controlled by accelerated mRNA degradation. PLoS Pathog. *10*, e1003882.

Adler, H., Messerle, M., Wagner, M., and Koszinowski, U.H. (2000). Cloning and mutagenesis of the murine gammaherpesvirus 68 genome as an infectious bacterial artificial chromosome. J. Virol. *74*, 6964–6974.

Anders, S., Pyl, P.T., and Huber, W. (2015). HTSeq—a Python framework to work with high-throughput sequencing data. Bioinformatics *31*, 166–169.

Braun, K.A., and Young, E.T. (2014). Coupling mRNA synthesis and decay. Mol. Cell. Biol. *34*, 4078–4087.

Brulois, K.F., Chang, H., Lee, A.S., Ensser, A., Wong, L.Y., Toth, Z., Lee, S.H., Lee, H.R., Myoung, J., Ganem, D., et al. (2012). Construction and manipulation of a new Kaposi's sarcoma-associated herpesvirus bacterial artificial chromosome clone. J. Virol. *86*, 9708–9720.

Covarrubias, S., Richner, J.M., Clyde, K., Lee, Y.J., and Glaunsinger, B.A. (2009). Host shutoff is a conserved phenotype of gammaherpesvirus infection and is orchestrated exclusively from the cytoplasm. J. Virol. *83*, 9554–9566.

Covarrubias, S., Gaglia, M.M., Kumar, G.R., Wong, W., Jackson, A.O., and Glaunsinger, B.A. (2011). Coordinated destruction of cellular messages in translation complexes by the gammaherpesvirus host shutoff factor and the mammalian exonuclease Xrn1. PLoS Pathog. *7*, e1002339.

Fuchs, G., Voichek, Y., Benjamin, S., Gilad, S., Amit, I., and Oren, M. (2014). 4sUDRB-seq: measuring genomewide transcriptional elongation rates and initiation frequencies within cells. Genome Biol. *15*, R69.

Gaglia, M.M., Covarrubias, S., Wong, W., and Glaunsinger, B.A. (2012). A common strategy for host RNA degradation by divergent viruses. J. Virol. *86*, 9527–9530.

Glaunsinger, B., and Ganem, D. (2004). Lytic KSHV infection inhibits host gene expression by accelerating global mRNA turnover. Mol. Cell *13*, 713–723.

Glaunsinger, B., Chavez, L., and Ganem, D. (2005). The exonuclease and host shutoff functions of the SOX protein of Kaposi's sarcoma-associated herpesvirus are genetically separable. J. Virol. *79*, 7396–7401.

Haimovich, G., Medina, D.A., Causse, S.Z., Garber, M., Millán-Zambrano, G., Barkai, O., Chávez, S., Pérez-Ortín, J.E., Darzacq, X., and Choder, M. (2013). Gene expression is circular: factors for mRNA degradation also foster mRNA synthesis. Cell *153*, 1000–1011.

Harel-Sharvit, L., Eldad, N., Haimovich, G., Barkai, O., Duek, L., and Choder, M. (2010). RNA polymerase II subunits link transcription and mRNA decay to translation. Cell *143*, 552–563.

Huch, S., and Nissan, T. (2014). Interrelations between translation and general mRNA degradation in yeast. Wiley Interdiscip Rev RNA *5*, 747–763.

Jagger, B.W., Wise, H.M., Kash, J.C., Walters, K.A., Wills, N.M., Xiao, Y.L., Dunfee, R.L., Schwartzman, L.M., Ozinsky, A., Bell, G.L., et al. (2012). An overlapping protein-coding region in influenza A virus segment 3 modulates the host response. Science *337*, 199–204.

Jinek, M., Coyle, S.M., and Doudna, J.A. (2011). Coupled 5′ nucleotide recognition and processivity in Xrn1-mediated mRNA decay. Mol. Cell *41*, 600–608.

Kamitani, W., Huang, C., Narayanan, K., Lokugamage, K.G., and Makino, S. (2009). A two-pronged strategy to suppress host protein synthesis by SARS coronavirus Nsp1 protein. Nat. Struct. Mol. Biol. *16*, 1134–1140.

Kwong, A.D., and Frenkel, N. (1987). Herpes simplex virus-infected cells contain a function(s) that destabilizes both host and viral mRNAs. Proc. Natl. Acad. Sci. USA *84*, 1926–1930.

Listerman, I., Sapra, A.K., and Neugebauer, K.M. (2006). Cotranscriptional coupling of splicing factor recruitment and precursor messenger RNA splicing in mammalian cells. Nat. Struct. Mol. Biol. *13*, 815–822.

Liu, S.Y., Sanchez, D.J., Aliyari, R., Lu, S., and Cheng, G. (2012). Systematic identification of type I and type II interferon-induced antiviral factors. Proc. Natl. Acad. Sci. USA *109*, 4239–4244.

Lotan, R., Goler-Baron, V., Duek, L., Haimovich, G., and Choder, M. (2007). The Rpb7p subunit of yeast RNA polymerase II plays roles in the two major cytoplasmic mRNA decay mechanisms. J. Cell Biol. *178*, 1133–1143.

Love, M.I., Huber, W., and Anders, S. (2014). Moderated estimation of fold change and dispersion for RNA-seq data with DESeq2. Genome Biol. *15*, 550.

Medina, D.A., Jordán-Pla, A., Millán-Zambrano, G., Chávez, S., Choder, M., and Pérez-Ortín, J.E. (2014). Cytoplasmic 5′-3′ exonuclease Xrn1p is also a genome-wide transcription factor in yeast. Front. Genet. *5*, 1.

Myoung, J., and Ganem, D. (2011). Infection of lymphoblastoid cell lines by Kaposi's sarcoma-associated herpesvirus: critical role of cell-associated virus. J. Virol. *85*, 9767–9777.

Nagarajan, V.K., Jones, C.I., Newbury, S.F., and Green, P.J. (2013). XRN 5′→3′ exoribonucleases: structure, mechanisms and functions. Biochim. Biophys. Acta *1829*, 590–603.

Phatnani, H.P., and Greenleaf, A.L. (2006). Phosphorylation and functions of the RNA polymerase II CTD. Genes Dev. *20*, 2922–2936.

Read, G.S. (2013). Virus-encoded endonucleases: expected and novel functions. Wiley Interdiscip Rev RNA *4*, 693–708.

Rice, S.A., Long, M.C., Lam, V., and Spencer, C.A. (1994). RNA polymerase II is aberrantly phosphorylated and localized to viral replication compartments following herpes simplex virus infection. J. Virol. *68*, 988–1001.

Richner, J.M., Clyde, K., Pezda, A.C., Cheng, B.Y., Wang, T., Kumar, G.R., Covarrubias, S., Coscoy, L., and Glaunsinger, B. (2011). Global mRNA degradation during lytic gammaherpesvirus infection contributes to establishment of viral latency. PLoS Pathog. *7*, e1002150.

Rowe, M., Glaunsinger, B., van Leeuwen, D., Zuo, J., Sweetman, D., Ganem, D., Middeldorp, J., Wiertz, E.J., and Ressing, M.E. (2007). Host shutoff during productive Epstein-Barr virus infection is mediated by BGLF5 and may contribute to immune evasion. Proc. Natl. Acad. Sci. USA *104*, 3366–3371.

Sugimoto, A., Sato, Y., Kanda, T., Murata, T., Narita, Y., Kawashima, D., Kimura, H., and Tsurumi, T. (2013). Different distributions of Epstein-Barr virus early and late gene transcripts within viral replication compartments. J. Virol. *87*, 6693–6699.

Sun, M., Schwalb, B., Schulz, D., Pirkl, N., Etzold, S., Larivière, L., Maier, K.C., Seizl, M., Tresch, A., and Cramer, P. (2012). Comparative dynamic transcriptome analysis (cDTA) reveals mutual feedback between mRNA synthesis and degradation. Genome Res. *22*, 1350–1359.

Sun, M., Schwalb, B., Pirkl, N., Maier, K.C., Schenk, A., Failmezger, H., Tresch, A., and Cramer, P. (2013). Global analysis of eukaryotic mRNA degradation reveals Xrn1-dependent buffering of transcript levels. Mol. Cell *52*, 52–62.

Trapnell, C., Pachter, L., and Salzberg, S.L. (2009). TopHat: discovering splice junctions with RNA-Seq. Bioinformatics *25*, 1105–1111.